Nanoscale Systems for Optical Quantum Technologies

Grant Agreement No: 712721
Start Date: 1st October 2016 - Duration: 36 months

D1.4 Optimized particles and thin films

Deliverable:	D1.4
Work package:	WP1 Nanomaterials, optical micro-cavities and control systems
Task:	1.1 Y_2O_3 nanoparticles development 1.2 Y_2O_3 thin films development
Lead beneficiary:	CNRS
Type:	Other
Dissemination level:	Public
Due date:	30 September 2018
Actual submission date:	30 September 2018
Author(s):	A. Ferrier, A. Tallaire, D. Serrano, P. Goldner (CNRS-CP)

This project has received funding from the European Union's Horizon 2020 research and innovation programme under grant agreement No 712721.

Version history

Version	Date	Author(s)	Description
V1	20/09/2018	A. Ferrier, A. Tallaire, D. Serrano (CNRS-CP)	Draft
V2	27/09/2018	A. Ferrier, A. Tallaire, D. Serrano, P. Goldner	Revised draft
V3	30/09/2018	A. Ferrier, A. Tallaire, D. Serrano, P. Goldner	Submission to EC

Table of Contents

Deliverable Description

In the present deliverable we report on the synthesis efforts carried out at CNRS-CP towards thin films and nanoparticles synthesis and optimization. In a first section devoted to rare-earth (RE) doped Y_2O_3 nanoparticles (RE^{3+}:Y_2O_3), we overview the samples produced up to now, underlying the progress which followed previous deliverables (D1.2 and D1.3). A particle size reduction below 100 nm has been achieved by a surfactant-assisted synthesis. The smallest particles synthesized so far (~ 60 nm) present homogeneous linewidths in the 100 kHz range. In a second section, we describe the first results obtained on the growth and on the spectroscopic characterizations of Y_2O_3 thin films doped with europium or erbium ions. This task is in close connection with Tasks 3.1-3.4 in which coupling between RE^{3+} and graphene or mechanical nano-resonators is investigated. Erbium or europium doped thin films with thicknesses of 10 to 300 nm have been grown by atomic layer deposition (ALD). We demonstrate that purity and crystallinity of the films is significantly improved by thermal post-processing. Structural and spectroscopic characterisations indicate that the optimal annealing temperature is 950°C, allowing to obtain films in which emission from rare-earth ions exhibits narrow inhomogeneous lines and long fluorescence lifetimes (T_1).

Nanoparticles

Introduction

Intensive synthesis and characterization work have been realized at CNRS-CP with the aim of providing optimum rare-earth doped nanoparticles. The requirements for particles are given by NanOQTech's WP2 tasks, including *Purcell enhancement of ion ensembles* (2.1), *Purcell-enhancement of a readout ion coupled to a qubit ion* (2.2), *Cavity-enhanced readout of ion-ion interactions* and *Cavity enhanced single photon emission at 1.5 μm* (2.3) and *Investigation of ion-ion interactions for quantum computation* (2.4). Strong collaboration between the partners enabled identifying the suitable rare-earth dopant, the optimum particle size and doping concentration, as well as the expected coherence properties for each task. A summary list of nanoparticles produced at CNRS-CP is given in **Table I**.

Table I: Summary of the nanoparticles samples currently under investigation. All samples with particles larger than 100 nm were produced by the fully-optimized homogenous precipitation method previously reported [1] and used in D1.2 and D1.3. A modified chemical route, 'surfactant-assisted homogeneous precipitation', was used for particles < 100 nm.

Sample	Concentration	Diameter	Partners	Tasks involved
Y_2O_3: Er^{3+}	200 ppm	150 nm	IRCP, ICFO-QP	Task 1.1, Task 2.3
Y_2O_3: Pr^{3+}	500 ppm	450 nm	IRCP, ICFO-QP	Task 1.1, Task 2.3
Y_2O_3: Pr^{3+}	500 ppm	150 nm	IRCP, ICFO-QP	Task 1.1, Task 2.3
Y_2O_3: Pr^{3+}-Nd^{3+}	1000 ppm – 1000 ppm	450 nm	IRCP, ULUND	Task 1.1, Task 2.2
Y_2O_3: Pr^{3+}-Nd^{3+}	500 ppm – 100 ppm	450 nm	IRCP, ULUND	Task 1.1, Task 2.2
Y_2O_3: Pr^{3+}-Nd^{3+}	500 ppm – 100 ppm	450 nm	IRCP, ULUND	Task 1.1, Task 2.2
Y_2O_3: Eu^{3+}	5000 ppm	450 nm	IRCP, KIT	Task 1.1, Task 2.1
Y_2O_3: Eu^{3+}	3000 ppm	450 to 60 nm[1]	IRCP, KIT	Task 1.1, Task 2.1

[1] Multiple batches of Eu^{3+} doped Y_2O_3 nanoparticles have been synthesized at CNRS-CP, with sizes ranging from 450 to 50 nm.

Pr^{3+} doped Y_2O_3 nanoparticles

Praseodymium (Pr^{3+}) ions present remarkable interest as an alternative to Eu^{3+} for quantum memories [3,4], quantum computing [5] and single photon emission [6] due to their larger oscillator strength and long optical and spin coherence lifetimes as demonstrated in Y_2SiO_5 bulk crystals [6,7]. Nevertheless, the coherence properties of the Pr^{3+}:$^1D_2 \leftrightarrow {}^3H_4$ optical transition, and that of the ground state hyperfine transitions in Y_2O_3 were up to date unknown. We report here the first investigation of the hyperfine structure and optical and spin coherence of $^{141}Pr^{3+}$ in Y_2O_3 ceramics and two sizes of nanoparticles (**Table I**). The ceramics were obtained by solid state reaction and have crystalline domains in the several micron range. They were used as highly scattering, self-supported thin slices (200 µm). They usually give longer coherence lifetimes and stronger signals than the nanoparticles powders. Optical coherence lifetime ($T_{2,opt}$) up to 6 µs was found in ceramics at 1.4 K. This value is longer than $T_{2,opt}$ measured in nanoparticles (**Fig. 1a** and **1b**) although still more than one order of magnitude shorter than values observed in the most performing bulk crystals [7]. In contrast, bulk-like spin coherence lifetimes were obtained both in ceramics and nanoparticles for the two ground state spin transitions identified at 10.42 MHz and 5.995 MHz (**Fig. 1c** and **1d**) [8]. These results are indeed comparable to those obtained in Eu^{3+}:Y_2O_3 nanoparticles [8,9, D1.3], therefore confirming the potential of $^{141}Pr^{3+}$ for the envisioned applications.

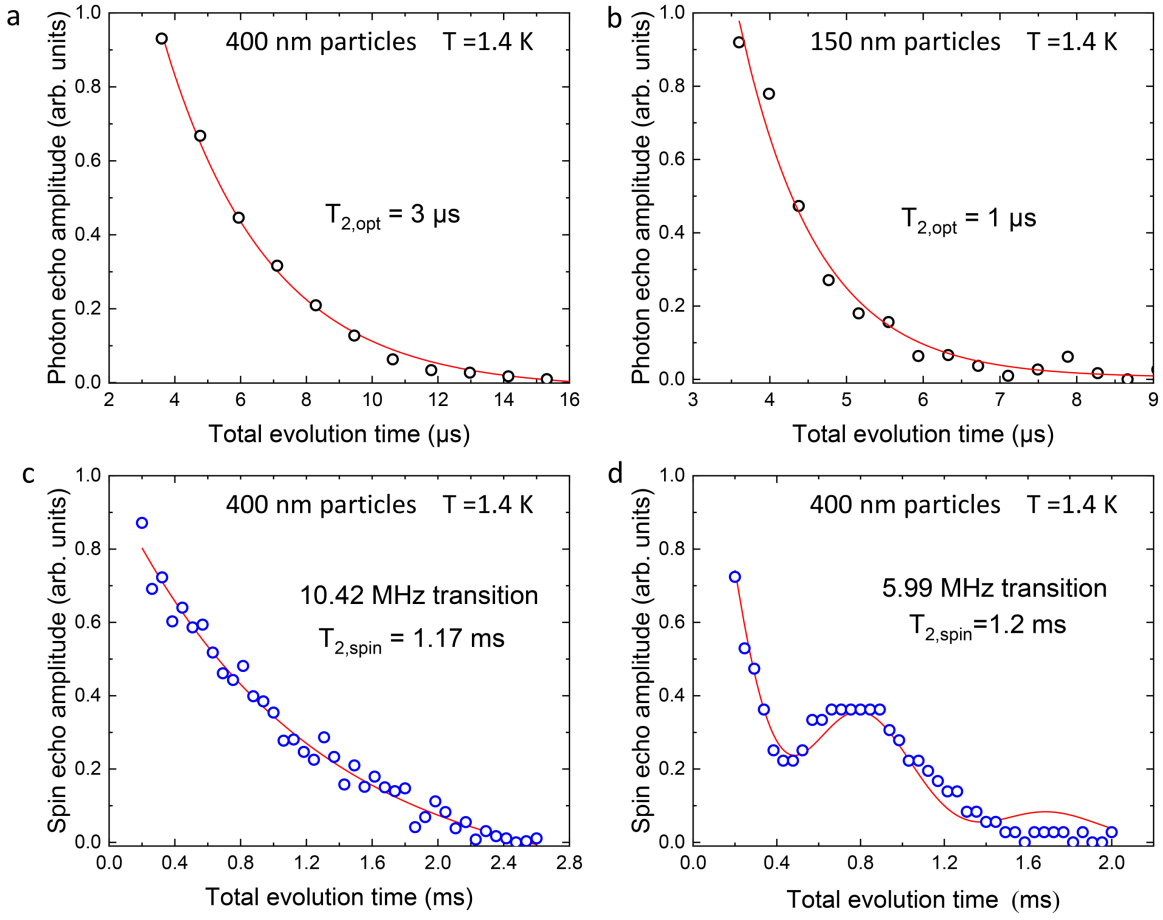

Figure 1: Optical and spin coherence investigations on Pr^{3+} doped Y_2O_3 nanoparticles (500 ppm doping) **a. and b.** Photon echo decay from the $^1D_2$-$^3H_4$ optical transition at 619.0075 nm (vac.) in 400 nm and 150 nm particles respectively. **c. and d.** Spin echo decay obtained from 400 nm particles for the 10.42 MHz and 5.99 MHz hyperfine transitions. The latter shows a clear

modulation similar to spin echo decays obtained in Eu^{3+}:Y_2O_3 ceramics [11]. All decays were fitted with a single exponential function but **d.,** which was fitted by a modulated exponential as in [11]**.**

Pr^{3+}-Nd^{3+} codoped Y_2O_3 nanoparticles

The codoping of Pr^{3+} with Nd^{3+} was concluded to be the most suitable for Task 2.2: *Purcell-enhancement of a readout ion coupled to a qubit ion*, lead by ULUND, as described in Deliverables D2.1 and D1.2. In the proposed scheme Pr^{3+} acts as a qubit ion and Nd^{3+} as a readout ion. Three batches of co-doped particles with different doping concentrations (**Table I**) are currently under investigation.

Er^{3+} doped Y_2O_3 nanoparticles

Erbium (Er^{3+}) doped Y_2O_3 nanoparticles are required for Task 2.3, namely "*Cavity enhanced single photon emission at 1.5 μm"*, lead by ICFO-QP. Preliminary photon echo measurements on Y_2O_3:Er^{3+} ceramics indicated that photon echoes could be recorded for an Er^{3+} doping concentration of 200 ppm at 2.7 K and in absence of external magnetic field. Following this investigation, 200 ppm Er^{3+} doped nanoparticles with an average size of 150 nm were synthesized (**Table I**). Such particle diameter is in principle suitable to ensure sufficient Purcell enhancement when coupling the particles to optical microcavities for the Er^{3+} transition wavelength at 1536 nm (D1.1).

Eu^{3+} doped Y_2O_3 nanoparticles

The main synthesis and research efforts towards longer optical and spin T_2 values and smaller nanoparticles carried out at CNRS-CP were carried out on europium (Eu^{3+}) doped Y_2O_3 nanoparticles. These particles have so far demonstrated the best coherence times [9,10] but are also those requiring the smallest size for efficient cavity coupling (~50 nm), see Task 2.1: *Purcell enhancement of ion ensembles*, led by KIT. Nevertheless, the methods developed at CNRS-CP to obtain smaller particles and extending the optical T_2 are not restricted to Eu^{3+} doped particles but can be successfully applied to any dopant. In other words, they are general to any rare-earth doped Y_2O_3 particles.

Deliverable D1.3 was exclusively devoted to the progress achieved on Eu^{3+} doped nanoparticles. We presented two possible strategies to reduce the particle size while achieving homogeneous linewidths of the order of 30 kHz and millisecond-long spin coherence times. These two strategies were direct chemical synthesis of small particles up to 150 nm, and the reduction of larger particles to smaller ones by chemical etching. In the present deliverable, we report subsequent progress in the direct chemical synthesis approach, therefore not included in previous reports. In particular, further particle size reduction down to 60 nm has been achieved by a modified homogeneous precipitation chemical route, namely surfactant-assisted route. The introduction of a surfactant has been previously reported to limit the particles growth [2,11] and is here necessary to keep the particles size below 100 nm. The route goes as follows: an appropriate amount of surfactant (PEG 8000 in this particular case) was dissolved in distilled water, and then mixed with urea ($CO(NH_2)_2$) and Eu/Y aqueous nitrate ($Eu(NO_3)_3$/$Y(NO_3)_3.xH_2O$) solutions. The concentrations were 4 g L^{-1}, 0.3-3 mol L^{-1} and 7.5 mmol L^{-1} for the surfactant, urea and metals (Eu^{3+} and Y^{3+}) respectively. The mixed solutions were then heated at 85 °C for 24 h in a Teflon reactor. After this reaction time, the suspensions were cooled to ambient conditions and the colloidal particles collected via centrifugation. The wet precipitates were washed with distilled water once to remove the byproducts, then

rinsed twice with absolute ethanol, and dried at 80 °C for 24 h to yield Eu^{3+}: $Y(OH)CO_3$ (YOC) amorphous particles. The Eu^{3+}:Y_2O_3 nanoparticles are finally obtained by annealing these YOC powders for 18 h at 800 °C under air atmosphere, with a heating rate of 3 °C min^{-1}. The particles were afterwards treated under oxygen plasma to cure impurities and/or defects. Standard annealing temperatures of 1200 °C, used for larger particles (see D1.3), led to strong sintering and aggregation for particles below 100 nm. For this reason, the calcination temperature was here kept at 800 °C but the annealing time was extended from the typical 6 h to 18 h. Transmission electron microscopy (TEM) images and the size distribution of particles obtained by this method are shown in **Figure 2**.

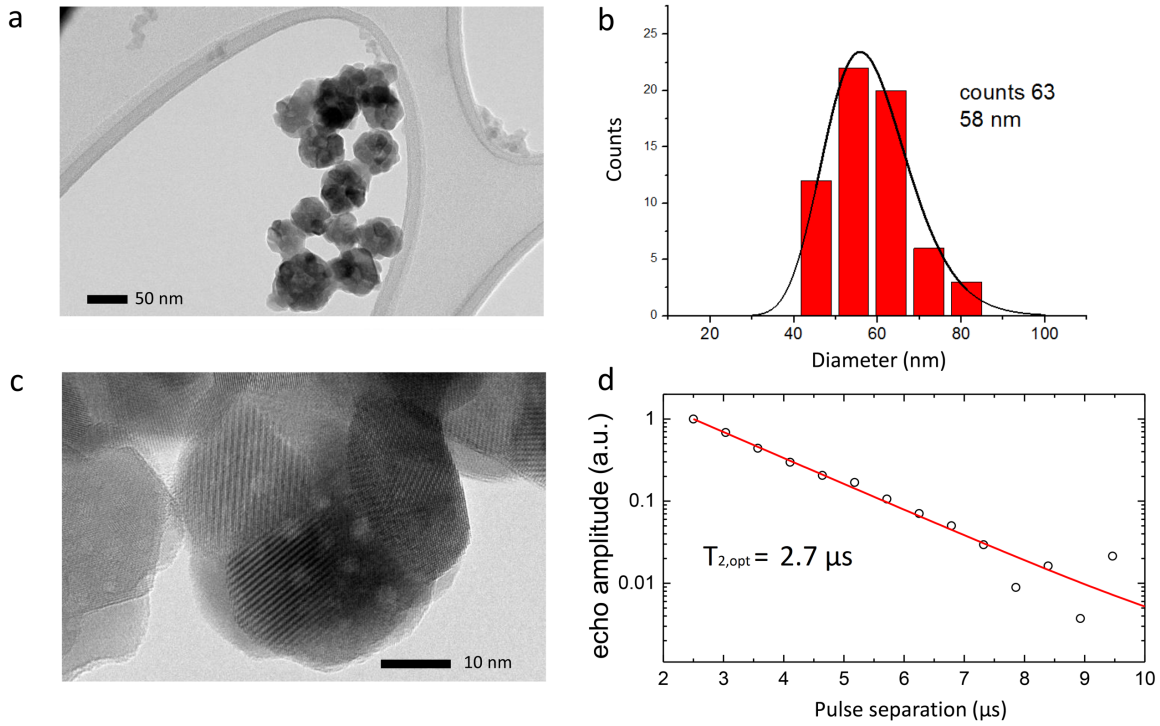

Figure 2: 60-nm-diameter particles obtained by surfactant-assisted synthesis. **a**. TEM image displaying polycrystalline particles. **b.** Particle size histogram. **c.** TEM image of the particle in which the crystalline sub-structures in the particle can be observed. **d.** Experimental two-pulse photon echo decay from these particles. $T_{2,opt}$ is derived from an exponential fit to the data.

After synthesis, two-pulse photon echo measurements were carried out in an ensemble of particles using the technique described in D1.3. The obtained photon echo decay, displayed in **Fig. 2d** yields an optical T_2 of 2.7 µs, equivalent to a homogeneous linewidth of 117 kHz. This result, obtained from particles annealed at 800 °C and presenting a crystalline grain size of around ~ 20 nm (**Fig. 2c**) is indeed outstanding, and constitutes a very important step towards NanOQTech's goals, especially those concerning Task 2.1. The grain size of the particles strongly depends on the annealing temperature [1]. For instance, 100-nm-diameter single-crystalline particles have been recently obtained by using a second annealing step at higher temperature (1200 °C) which avoids aggregation issues (**Fig. 3**). Further optimization of the annealing step for the 60-nm-particles is therefore planned as well as more optical characterizations to get further insight into the influence of the crystalline grain size on the optical coherence performance of the particles.

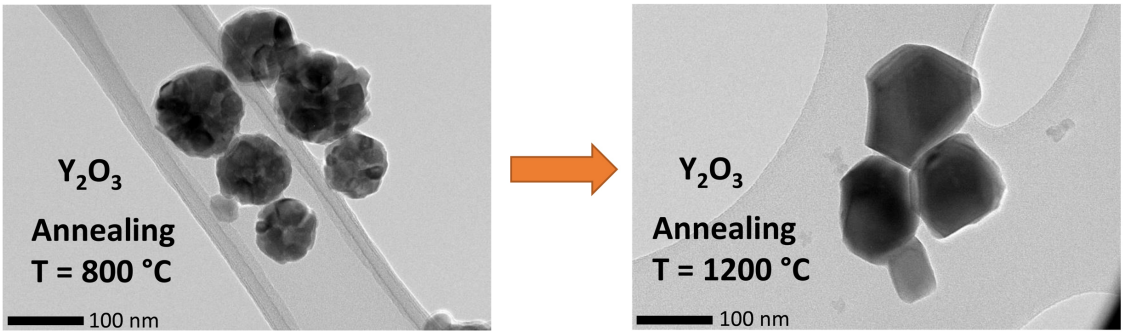

Figure 3: Effect of the post-synthesis annealing on the crystalline grain size. Polycrystalline Y_2O_3 particles are obtained under 800 °C annealing of the YOC raw material. A second annealing step at 1200 °C yield single crystal particles, with characteristic sharp facets.

Thin films

Introduction

Sesquioxide thin films can be grown by a wide range of methods to address several applications, e. g. high κ materials for micro-electronics, protective or super hydrophobic coatings [13,14]. Among the different synthesis methods, Atomic Layer Deposition (ALD) appears promising, allowing high conformity and an atomic scale control over the thickness [14]. Although several studies have dealt with RE:Y_2O_3 growth by ALD for photonics applications [15, 16] no report on high resolution and coherent spectroscopy exists so far. NanOQTech's efforts have thus focused on the optimization of the film deposition process with a direct feedback from structural and spectroscopic analyses. These developments aim at providing high-performance samples for Tasks 3.1-3.4, in which hybrid devices, using graphene or mechanical nano-resonators, are investigated.

Methods

Yttria films were deposited with a *Picosun Sunale R200* vertical flow type reactor using commercial RE(tmhd)$_3$ precursors (STREM chemicals) and ozone as an oxidizing source. High purity N_2 was used as a carrier and purge gas. The temperature of the reactor was set between 250°C and 400°C. In order to determine the best deposition conditions, we tested the effect of ozone and N_2 purge pulse duration, as well as the deposition temperature. The film quality has been assessed by combined XRD analysis and photoluminescence experiments (see below). From this study, the optimal ALD sequence consisted of a 3 s Y(tmhd)$_3$ pulse followed by a 3 s purging pulse of N_2; a 3 s ozone pulse also followed by a 3 s N_2 purge (**Fig. 4a**). For a doping level of 5 %, the Y precursor pulse was replaced by 15 pulses of Eu^{3+} or Er^{3+} precursor every 300 cycles. The self-limited regime was obtained for moderate temperatures of around 200-400°C with large-scale uniformity (**Fig. 4c**). Indeed, in this temperature range the film thickness increases linearly at about 0.22 Å per cycle (**Fig. 4b**).

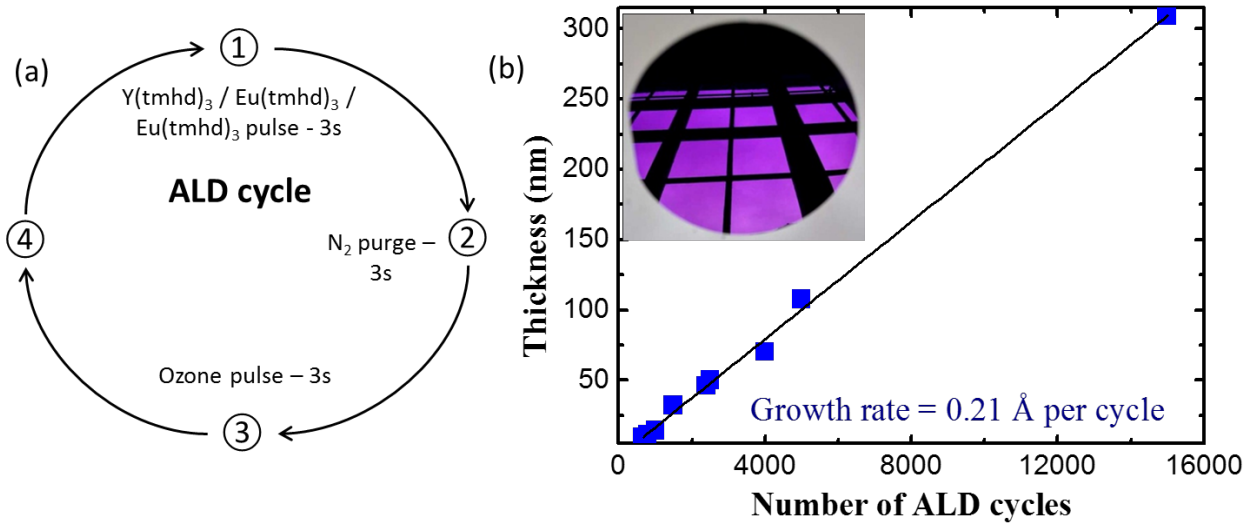

Figure 4 (a) A typical ALD cycle used to grow the Y_2O_3 thin films. **(b)** Film thicknesses measured by white light interferometry as a function of cycle number. Inset: image of a 2 inches Si wafer covered by a uniform Y_2O_3 ALD coating and showing a mirror-like behaviour.

Structural and morphological characterization

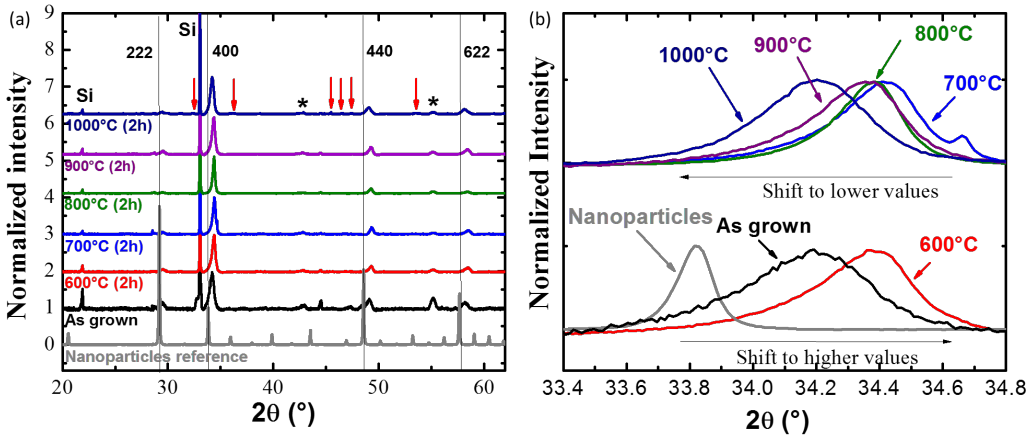

Figure 5: **(a)** XRD pattern, normalized to the (400) diffraction peak, of Er^{3+}:Y_2O_3 films annealed at different temperatures. The films' thickness is 300 nm. Y_2O_3 cubic phase nanoparticles is used as a reference. The red arrows underline the appearance of parasitic phases **(b)** Evolution of the (400) diffraction peak position with annealing temperature.

The structural characterization of the deposited yttria thin films was carried out on an X-ray diffractometer (*Panalytical X'Pert*) using Cu $K\lambda_1$ wavelength. XRD analysis of films annealed at different temperatures is presented in **Fig. 5** and compared with Y_2O_3 cubic nanoparticles obtained by homogeneous precipitation. The agreement between the reference powder and the films diffraction peaks (**Fig. 5a**) indicates that polycrystalline Y_2O_3 have been grown mostly in the cubic phase. The relative intensity of the different peaks with respect to the randomly oriented nanopowders shows preferentially oriented

growth along the (400) crystallographic planes. The peak diffraction intensity increases significantly when a post growth annealing treatment is performed underlying significant improvement of the crystallinity. However, for 1000 °C annealing, additional peaks appear (red arrows in **Fig. 5a**). These peaks are due to the formation of parasitic silicate phases (such as Y_2SiO_5 or $Y_2Si_2O_7$) indicating solid-state reaction between the yttria film and the silicon wafer. This reaction sets an upper limit for the annealing temperature. In addition, a small shift of the diffraction peaks is observed most likely because of the lattice unit cell and thermal expansion coefficient mismatches between silicon and yttria [17, 18]. The induced stress sometimes leads to cracking for the thickest films annealed at the highest temperatures. However, 100 nm or thinner oxide films annealed up to 950°C do not exhibit cracks or parasitic phase formation which is encouraging for their future integration in a device.

Optical properties

The optical properties of erbium and europium ions doped in Y_2O_3 have been studied by photoluminescence (PL). PL measurements were performed using a Renishaw micro-PL apparatus with a 20 X objective and a 532 nm laser as the excitation source. The room temperature PL spectra as a function of the annealing treatment are presented in **Figure 6**. They are dominated by the $^5D_0 \rightarrow {}^7F_2$ emission at 612 nm (**Fig. 6a** and **6b**) corresponding to ions in the C_2 site of the cubic structure of yttria. For as-grown films or films annealed at low temperatures, an additional contribution from the same electronic transition but for ions in the monoclinic Y_2O_3 phase is visible around 622 nm. When increasing the annealing temperature, this emission tends to disappear. A significant increase in the luminescence intensity associated with a narrowing of the peaks is observed for the annealed samples (Fig. **6c** and **6d**). This confirms the significant improvement in the crystalline environment around RE ions. The thermal post treatment has a double effect: until 800°C, a significant increase of the integrated intensity is observed which indicates a reduction of defects and impurities in the film. From 800°C to 950°C the integrated intensity remains the same but the peak at 612 nm becomes more intense and narrow (**Fig. 6c** et **6d**). In this range of temperature, a significant improvement of the crystalline environment of the RE ions is therefore deduced. Above 1000°C, a decrease in the integrated luminescence and the apparition of new emission lines confirm the formation of additional crystalline phases. The optimal annealing temperature is thus 950°C.

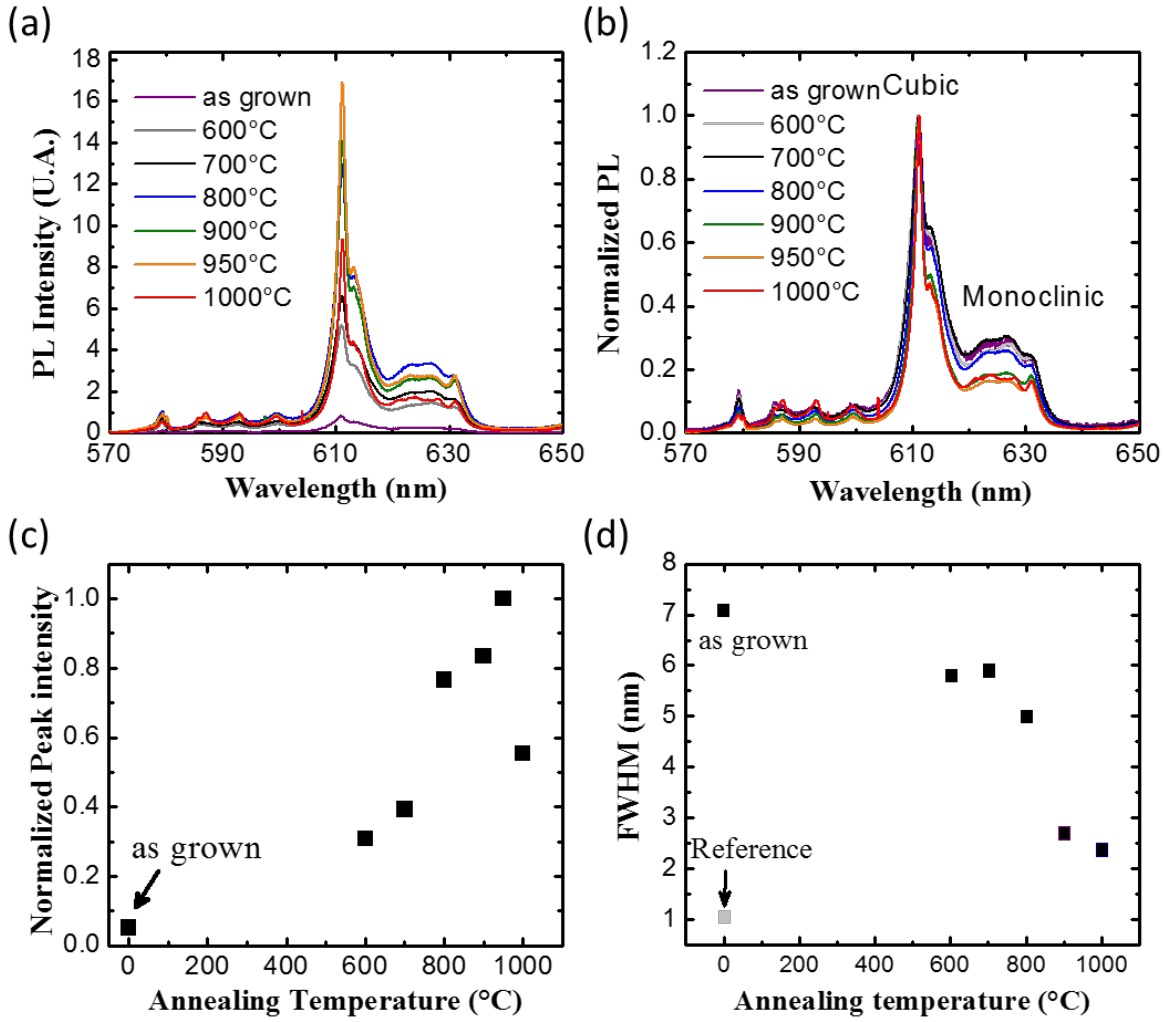

Figure 6 (a) Room-temperature PL spectra (normalized at 612 nm in **(b)**) of 100 nm-thick Y_2O_3 films doped with 5 % Eu^{3+} showing the main Eu emission lines in a cubic or monoclinic environment. **(c)** Variation of the PL intensity maximum at 612 nm as a function of the annealing temperature. The values have been normalized to the maximum PL emission at 950 °C. **(d)** Full width at half maximum of the $^5D_0$ - $^7F_2$ transition at 612 nm plotted as a function of annealing temperature. The value obtained from a ceramic with the same composition is used as a reference.

The inhomogeneous linewidth (Γ_{inh}) represents the frequency distribution of an ensemble of emitters and is a useful indicator of the RE ions close environment. Indeed, the static disorder or the defects in the surrounding of the europium ions influence the width, peak position and line shape of the transitions. Measuring Γ_{inh} in thin films is challenging because of the low oscillator strength of the $^5D_0$ - $^7F_0$ transition and the small number of RE ions in a sub-micron film. We nevertheless determined the $^5D_0$ - $^7F_0$ transition Γ_{inh} in reflection mode in a helium bath cryostat (*Janis SVT-200*) between 10 and 12 K. A low laser intensity (1 mW) was used to avoid saturation of the transition and spectral hole burning. We performed fluorescence excitation experiments by monitoring the red luminescence of the $^5D_0 \rightarrow {}^7F_2$ transition while scanning a *Sirah Matisse DS dye laser*, with a linewidth of 200 kHz, around 580.883 nm (516 098 GHz). The red luminescence is detected using at least 3 band pass filters and send to a high sensitivity photomultiplier (*Hamamatsu R5108*). In order to improve the signal to noise ratio of the detection, we

used a lock-in amplifier (*Perkin Elmer 5210*). The excitation spectra of four films annealed at different temperature are presented in **Figure 7**. Two main contributions are observed around 518 400 GHz (Peak B) and 516 150 GHz (Peak A). The central frequency of peak A is in good agreement with the C_2 site of the cubic Y_2O_3 whereas peak B is attributed to the monoclinic phase. Again, the benefits of the annealing post treatment clearly appears since a significant increase of peak A intensity is observed with the increase in post treatment temperature. Γ_{inh} for peak A is around 200 GHz and remains larger than those of nanocrystals doped with 5% of Eu^{3+} and annealed at 1200°C (130 GHz). This suggests that the linewidth in the films is only partly due to the mismatch between Eu^{3+} and Y^{3+} ionic radii and that additional disorder, defect or impurities also contribute to it. A blue shift of the peak maximum is also observed with the increase of the annealing temperature which we attribute to tensile stress [19]. This is consistent with previous XRD measurements.

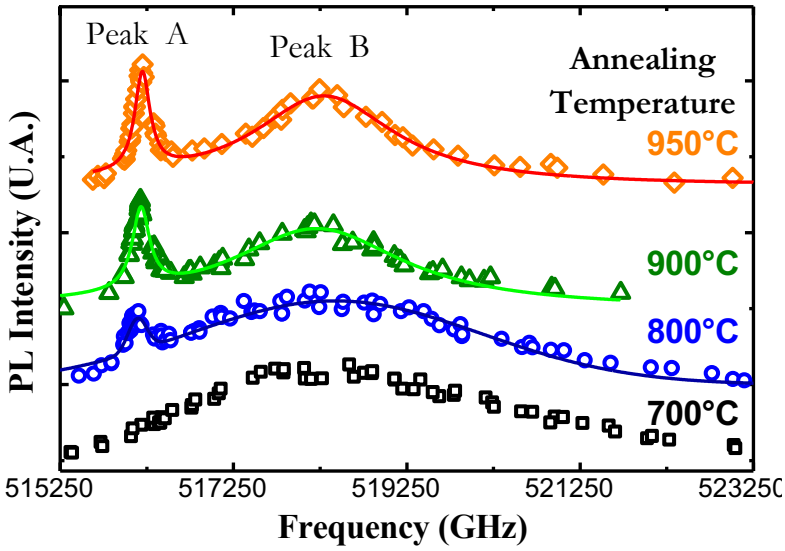

Figure 7: Inhomogeneous absorption line at 10 K of the $^7F_0 \rightarrow {}^5D_0$ transition of Eu^{3+} ions in Y_2O_3 ALD thin films for different annealing temperatures. Films are 300 nm thick and doped with 5% Eu. Emission of the $^5D_0 \rightarrow {}^7F_2$ transition is monitored at wavelengths above 610 nm as a function of the laser excitation frequency to probe the $^7F_0 \rightarrow {}^5D_0$ transition. The solid line is a fit of the experimental points with two Lorentzian line shapes. Curves have been vertically shifted for clarity.

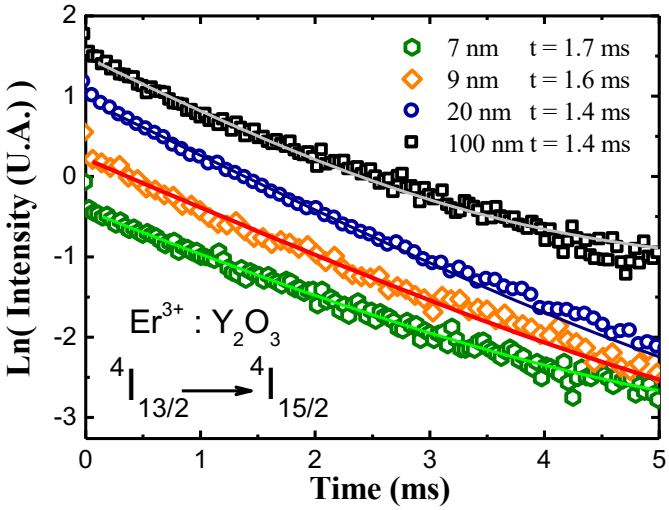

Figure 8: Decay curves of the 1.5 µm fluorescence of Er^{3+} ions (2 %) doped into a Y_2O_3 film annealed at 950°C. Open symbols: experimental points, solid lines: single exponential fit. For clarity, curves have been vertically shifted

Finally, we also studied, in close collaboration with ICFO-QP, the possibility to dope RE optical emitters into a very thin oxide film to study their coupling to graphene (in connection with Tasks 3.1 and 3.2). The effect of the film thickness on the luminescence lifetime of the 1.5 µm transition of Er^{3+} is presented in **Figure 8**. All the films have been annealed at the optimal temperature of 950°C. Time-decay measurements showed that millisecond long fluorescence lifetimes of the first excited state of Er^{3+} ions can be observed in these samples. Indeed, quasi exponential decays are measured with a time constant of about 1.5 ms. Those lifetimes are shorter than the 7.7 ms measured for a 1% Er^{3+}:Y_2O_3 transparent ceramic but are remarkably long in comparison with the values obtained in 10 nm nanocrystals (<100 µs) [20].

Conclusion

In summary, we have reached the particle size objective for Eu^{3+} doped nanoparticles for coupling to optical microcavities and demonstrated that optical homogeneous linewidths on the order of 120 kHz are achievable at such small sizes. Post-growth annealing treatments at high temperatures are currently under investigation and are expected to further narrow the linewidths. We also determined the hyperfine structure of the $^{141}Pr^{3+}$ isotope in Y_2O_3 and measured for the first time optical and spin coherence lifetimes, confirming the great potential of this material system for the quantum technologies targeted in NanOQTech. In addition, Pr^{3+}-Nd^{3+} co-doped and Er^{3+} doped nanoparticles have been synthesized following the requirements identified for Tasks 2.2 and 2.3.

We have optimized the growth of Eu^{3+} and Er^{3+} doped Y_2O_3 thin films by ALD and evaluated their optical properties. The use of adapted growth conditions and post-growth thermal annealing shows that high quality, homogeneous films with narrow and well-resolved emission lines can be produced. Annealing temperatures on silicon were limited to about 950 °C in order to obtain the best spectroscopic properties without the formation of parasitic silicate phases or cracks on the surface. We demonstrated that two different environments exist around europium ions. Based on the central frequency of the $^5D_0$-$^7F_0$ line, we conclude that the films consist of a dominant cubic phase with a minor

contribution from a disordered monoclinic phase. By annealing, a conversion of the monoclinic phase to the cubic phase is observed with an optimal temperature of 950°C. Despite this phase mixing, we observed a narrow inhomogeneous linewidth, close to the bulk value, for ions in the cubic phase. Finally, we demonstrated that the 1.5 µm emission of erbium can be observed for sub 10 nm thick films grown under optimized conditions and after post treatment. Long lifetimes of 1.5 ms were measured, indicating a low concentration of quenching centres. This opens the way to spatially localize rare-earth emitters in very thin ALD films (10 nm), which is needed for coupling to graphene (Tasks 3.1 and 3.2) and mechanical nano-resonators (Tasks 3.3 and 3.4). However, at this stage, further study of RE ions coherent properties is needed.

References

[1] K. de Oliveira Lima, R. Rocha Gonçalves, D. Giaume, A. Ferrier, et P. Goldner, « Influence of defects on sub-Å optical linewidths in Eu3+: Y2O3 particles », *J. Lumin.*, vol. 168, p. 276-282, 2015.

[2] H. Wang, P. Liu, X. Cheng, A. Shui, et L. Zeng, « Effect of surfactants on synthesis of TiO2 nano-particles by homogeneous precipitation method », *Powder Technol.*, vol. 188, nº 1, p. 52-54, 2008.

[3] G. Heinze, C. Hubrich, et T. Halfmann, « Stopped Light and Image Storage by Electromagnetically Induced Transparency up to the Regime of One Minute », *Phys. Rev. Lett.*, vol. 111, nº 3, p. 033601, 2013.

[4] M. Gündoğan, P. M. Ledingham, K. Kutluer, M. Mazzera, et H. de Riedmatten, « Solid State Spin-Wave Quantum Memory for Time-Bin Qubits », *Phys. Rev. Lett.*, vol. 114, nº 23, p. 230501, 2015.

[5] L. Rippe, B. Julsgaard, A. Walther, Y. Ying, et S. Kröll, « Experimental quantum-state tomography of a solid-state qubit », *Phys. Rev. A*, vol. 77, nº 2, p. 022307, févr. 2008.

[6] E. Eichhammer, T. Utikal, S. Götzinger, et V. Sandoghdar, « Spectroscopic detection of single Pr 3+ ions on the 3 H 4 − 1 D 2 transition », *New J. Phys.*, vol. 17, nº 8, p. 083018, 2015.

[7] R. W. Equall, R. L. Cone, et R. M. Macfarlane, « Homogeneous broadening and hyperfine structure of optical transitions in Pr^{3+}:Y_2SiO_5», *Phys. Rev. B*, vol. 52, nº 6, p. 3963-3969, 1995.

[8] E. Fraval, M. J. Sellars, et J. J. Longdell, « Method of Extending Hyperfine Coherence Times in Pr^{3+}:Y_2SiO_5», *Phys. Rev. Lett.*, vol. 92, nº 7, p. 077601, 2004.

[9] J. G. Bartholomew, K. de Oliveira Lima, A. Ferrier, et P. Goldner, « Optical Line Width Broadening Mechanisms at the 10 kHz Level in Eu3+:Y2O3 Nanoparticles », *Nano Lett.*, vol. 17, nº 2, p. 778-787, 2017.

[10] D. Serrano, J. Karlsson, A. Fossati, A. Ferrier, et P. Goldner, « All-optical control of long-lived nuclear spins in rare-earth doped nanoparticles », *Nat. Commun.*, vol. 9, nº 1, p. 2127, 2018.

[11] J. Karlsson, N. Kunkel, A. Ikesue, A. Ferrier, et P. Goldner, « Nuclear spin coherence properties of 151 Eu 3+ and 153 Eu 3+ in a Y 2 O 3 transparent ceramic », *J. Phys. Condens. Matter*, vol. 29, nº 12, p. 125501, 2017.

[12] N. Uekawa, M. Ueta, Y. J. Wu, et K. Kakegawa, « Characterization of CeO2 Fine Particles Prepared by the Homogeneous Precipitation Method with a Mixed Solutionof Ethylene Glycol and Polyethylene Glycol », *J. Mater. Res.*, vol. 19, nº 4, p. 1087-1092, 2004.

[13] G. Azimi, R. Dhiman, H.-M. Kwon, A. T. Paxson and K. K. Varanasi, « Hydrophobicity of rare-earth oxide ceramics », *Nature materials*, 12, p. 315–320, 2013.
[14] M. Leskela et al., «Rare-earth oxide thin films for gate dielectrics in microelectronics », *J. of alloys Compounds,* 418, p 27, 2006
[15] J. Hoang, R. N. Swartz, K.L. Wang, P. J. Chang, « Er^{3+} interlayer energy migration as the limiting photoluminescence quenching factor in nanostructured Er^{3+}:Y_2O_3 thin films », *J. Appl. Phys.,* 112, p 023116, 2012.
[16] T. T. Van and P. J. Chang, « Controlled Er^{3+} incorporation and photoluminescence of Er^{3+} : Y_2O_3 thin films », *Appl. Phys. Lett.,* 87, p 011907, 2005 .
[17] S.C Choi et al., « Heteroepitaxial growth of Y_2O_3 films on silicon », *Appl. Phys. Lett.,* 71, p 903, 1997.
[18] J. W. Palko et al., « Elastic constants of Yttria (Y_2O_3) monocrystals to high temperatures" », *J. Appl. Phys.,* 89, p 7791, 2001.
[19] Z. Li et al., « Analysis of the up-conversion photoluminescence spectra as a probe of local microstructure in Y_2O_3 Eu^{3+} nanotubes under high pressure *RSC Adv*. », 5, p. 3130, 2015.
[20] J. A. Dorman et al. « Elucidating the effects of a Rare Earth oxide shell on the luminescence of Er^{3+}:Y_2O_3 nanoparticles »*, J. Phys. Chem. C*, 116, p. 10333, 2012.